

# Electronic structure and optical properties of ZnS/CdS nanoheterostructures

J. Pérez-Conde

*Departamento de Física, Universidad Pública de Navarra, E-31006, Pamplona, Spain*

A. K. Bhattacharjee

*Laboratoire de Physique des Solides, UMR du CNRS, Université Paris-Sud, F-91405, Orsay, France*

The electronic and optical properties of spherical nanoheterostructures are studied within the semi-empirical  $sp^3s^*$  tight-binding model including the spin-orbit interaction. We use a symmetry-based approach previously applied to CdSe and CdTe quantum dots. The complete one-particle spectrum is obtained by using group-theoretical methods. The excitonic eigenstates are then deduced in the configuration-interaction approach by fully taking into account the Coulomb direct and exchange interactions. Here we focus on ZnS/CdS, ZnS/CdS/ZnS and CdS/ZnS nanocrystals with particular emphasis on recently reported experimental data. The degree of carrier localization in the CdS well layer is analyzed as a function of its thickness. We compute the excitonic fine structure, i.e., the relative intensities of low-energy optical transitions. The calculated values of the absorption gap show a good agreement with the experimental ones. Enhanced resonant photoluminescence Stokes shifts are predicted.

The quantum confinement effects in semiconductor nanocrystals (NC's) or quantum dots (QD's) have been investigated over the last two decades. A recent development concerns nanoheterostructures containing concentric layers of two different semiconductors. The initial idea of capping a NC with a shell of higher-gap (barrier) material in order to reduce the uncontrolled surface effects has been extended to quantum-dot quantum-well (QDQW) structures with an inner layer of lower-gap (well) material which allow a greater control over the optical properties.[1] There are several examples such as the inclusion of a layer of HgS in a CdS NC [1, 2, 3], where the lattice parameters of both compounds are of similar size ( $a = 5.851 \text{ \AA}$  for the  $\beta$ -HgS and  $a = 5.818 \text{ \AA}$  for the CdS). Recently, ZnS/CdS based QDQW's have been synthesized [4, 5] with a larger lattice mismatch (more than 7 % , the ZnS lattice constant being  $a = 5.409$ ). Some other combinations have also been studied, such as CdSe/ZnS [6] or CdSe/CdS.[7]

On the theoretical side, effective mass approximation (EMA) models were proposed [2, 8] without a full many-body treatment of the Coulomb direct and exchange interactions. An atomistic theory was needed, however, to adequately describe a QDQW where the well can be as thin as one monolayer. Very recently we proposed a tight-binding (TB) model [9], which is a generalization of our previous work. This theory successfully accounted for the optical properties of CdSe [10] and CdTe [11, 12] NC's. Independently, Bryant and collaborators have also developed a TB approach. [4, 13] In contrast with the Bryant group, we include the spin-orbit interaction, take into account the symmetries and obtain the full single-particle spectrum before deducing the exciton states. The Coulomb and exchange interactions were already incorporated in our study of CdS/HgS/CdS QDQW's[9], prior to the more recent work by Xie *et al.*[14] To our knowledge, the present paper reports the first TB calculation of the low-energy excitonic states in CdS/ZnS nanoheterostructures. After a brief description of the

theoretical model which can be completed with our previous publications [9, 10, 12], we present our main results on ZnS/CdS, ZnS/CdS/ZnS and CdS/ZnS nanocrystals, including a comparison with the available experimental data.

Our calculations are based on the semi-empirical TB model for bulk semiconductors introduced by Vogl *et al.* [15] and generalized by Kobayashi *et al.* to account for the spin-orbit interaction.[16] In this model five atomic orbitals are used:  $s$ ,  $p_x$ ,  $p_y$ ,  $p_z$ ,  $s^*$ . The phenomenological  $s^*$  orbital was introduced in order to simulate the effects of  $d$  orbitals on the conduction bands. The interatomic hopping matrix elements are restricted to the nearest neighbors. The model is then described by a total of 15 independent parameters. The CdS TB parameters used here are essentially those proposed earlier by Lippens and Lannoo [17] which we have slightly modified in order to incorporate the spin-orbit coupling. The ZnS parameters are those calculated by Bertho.[18] As for the band offset, following Ref. [4], the valence band maximum of ZnS is set to 0 eV and that of CdS shifted to +0.4 eV. The bulk gaps of ZnS and CdS are 3.7 eV and 2.5 eV respectively.

We outline the method for deriving the symmetrized TB Hamiltonian (see Ref. 12 for details). The NC's, of roughly spherical shape, are constructed starting from a cation at the origin by successively adding nearest-neighbor atoms through tetrahedral bonding. We passivate the NC surface by placing a hydrogen  $s$  orbital at each empty nearest-neighbor site on the surface dangling bond so that the final surface states are several eV far from the gap edges. Hereafter we use a simplified notation: We write  $r_{co}/r_w/r_{cl}$  to indicate that a NC is built with a core radius  $r_{co}$ , with  $r_w$  and  $r_{cl}$  designating the widths of the well and clad layers, respectively. The lengths are all given in angstroms.

The single-particle TB Hamiltonian is reduced to a block diagonal form by writing it in a symmetrized basis corresponding to the double-valued representations

$\Gamma_k$  ( $k = 6, 7, 8$ ) of the  $T_d$  point group.[19] This method not only reduces the size of the Hamiltonian to diagonalize, but also provides the exact symmetry classification of the wavefunctions. One can thus deduce selection rules and related insights over the relative intensities of optical transitions between the valence and conduction states.[12] We then diagonalize the Hamiltonian and obtain the full one-particle spectrum in a given nanostructure: all the energy levels and eigenstates. We have also calculated the spatial projections of the density of states (DOS) onto the core, well and clad regions, when required, to study the influence of the position and thickness of different layers on the whole energy spectrum.

The optical properties concern exciton-like elementary excitations which can be described in terms of the Coulomb direct and exchange interactions between the electron and hole. The total Hamiltonian can be written as, [10]

$$H_{vc,v'c'} = (\varepsilon_c - \varepsilon_v)\delta_{vv'}\delta_{cc'} - J_{vc,v'c'} + K_{vc,v'c'}, \quad (1)$$

where  $\varepsilon_c$ ,  $-\varepsilon_v$  are the electron and hole energies,  $J$  and  $K$  are the Coulomb and exchange interactions respectively (see Ref. 10 for more details). Note that we leave the  $e-h$  exchange interaction ( $K$ ) unscreened up to the nearest-neighbor site (primitive cell of the zincblende crystal), in analogy with the unscreened short-range part in the theory of bulk exciton.

The unscreened on-site Coulomb and exchange integrals for anion (cation) are assumed to be  $U_{coul} = 20(6.5)$  eV and  $U_{exch} = 1(0.5)$  eV respectively. These values follow roughly those obtained for CdSe and CdTe. [10, 20] The values for the S atom in CdS have been calculated by means of a simple scaling. We assume the same parameters for ZnS. The nearest-neighbor exchange integrals are assumed one tenth of the on-site ones. The permittivity is taken as  $\epsilon(\infty)$ :  $\epsilon(\infty) = 5.7$  for ZnS and  $\epsilon(\infty) = 5.2$  for CdS in single binary QD's. We take an average value in ZnS/CdS,  $\epsilon(\infty) = 5.4$ . Strictly speaking, the dielectric constant in a nanocrystal is size-dependent and substantially reduced with respect to the bulk low-frequency value  $\epsilon(0)$ . See, for example, Ref. [21], where a pseudopotential calculation for CdSe nanocrystals is presented: The dielectric constant increases with increasing size and asymptotically approaches the bulk high-frequency value  $\epsilon(\infty)$ . To our knowledge, no such calculations are available for the present nanoheterostructures nor even for their components. We, therefore, assume an average of the bulk high-frequency values.

The large lattice mismatch in the ZnS/CdS system is expected to lead to elastically strained structures with the relatively thin shell/well layers conforming to the substrate lattice constant.[4] Unfortunately, there is no simple way of including this effect in our TB model. Preliminary calculations suggest that a simple modification of the interatomic matrix elements alone, following the Harrison scaling rule for the bond length, is inadequate: It yields a systematic increase of the optical gap in the ZnS/CdS and ZnS/CdS/ZnS structures considered here

by 10-30 %. The effect is, of course, qualitatively inverse in CdS/ZnS. A more refined modelization scheme for structural distortion involving the diagonal matrix elements (see, for example, Ref.[22]) seems necessary. Work is in progress in this direction and will be reported elsewhere. The results presented below have been obtained by neglecting the strain effects.

In Fig. 1 we show the total density of states for some ZnS, CdS and ZnS/CdS/ZnS NC's. It can be seen how the projection of DOS onto the CdS well quickly grows when one and two monolayers are added. A monolayer yields a CdS well projection, almost equivalent in size and energy distribution, to the core ZnS projection. The addition of a second layer leads to a CdS well projection which is much larger than the corresponding ZnS projection. Interestingly, the size of the gap is governed essentially by the ZnS properties. We also look at the radial distribution of charge corresponding to the eigenstates. We can see the numerical values of the probability of presence of electron and hole in the LUMO and HOMO in Table I for several cases. The idea behind the comparison is to investigate the role of the successively added CdS layers. Both the electron and hole show an enhancement of their presence in the well region; the effect is more pronounced for the hole. When two CdS layers are added the hole is essentially trapped in the well. In Table II we show the two highest valence (HOMO) and two lowest conduction (LUMO) levels. The ZnS single-particle spectrum presents an intrinsic degeneracy which is the consequence of the absence of spin-orbit coupling: When a level is  $\Gamma_7 - \Gamma_8$  degenerate its orbital symmetry is  $\Gamma_5$ , because the spin-1/2 representation is  $\Gamma_6$  and  $\Gamma_5 \times \Gamma_6 = \Gamma_7 + \Gamma_8$ . Similarly, the degeneracy  $\Gamma_6 - \Gamma_8$  indicates that the underlying orbital symmetry is  $\Gamma_4$ .

The excitonic spectrum is calculated by diagonalizing the exciton Hamiltonian in Eq. (1) in the configuration-interaction method with as many valence and conduction states as necessary to reach numerical convergence. The relative intensities of optical transitions are next computed by following the procedure described in Ref. [10].

In order to discuss the available experimental data, let us first note that in QDQW structures like CdS/ZnS: in Ref. [5] the dispersion for dots with a mean diameter of  $58 \text{ \AA}$  is  $\sigma = 9 \text{ \AA}$ . On the other hand, in small nanocrystals, theoretical results show big jumps in the energies when one adds just one or two shells to a given NC: See Table II. Our procedure to fix the adequate size for a given set of experimental data [4] is as follows: We first analyze several NC's of sizes differing by one or two atomic shells around the experimental size and retain three such structures yielding a good agreement with the experimental values of size and optical absorption gap. The procedure is illustrated in Fig. 2: We show the fine structure of absorption for three different ZnS NC's of around  $20 \text{ \AA}$  diameter. We can see that the experimental onset from [4], indicated by a vertical dashed line, is in good agreement with our results if we remember that the onset must have a finite width. Note that the succes-

sive sizes in Fig. 2 correspond to the addition of single atomic shell. In Fig. 3 we show the fine structure of a series of QDQW's based on a ZnS core of radius 7.2 Å. The experimental values are given in the figure caption. Finally, it is worth mentioning that the predicted photoluminescence Stokes shift is enhanced by the presence of the barriers. In particular, the Stokes shift in the  $R = 14.8$  Å CdS NC is 12 meV, whereas the 7.2/5.9/2.6 QDQW, even slightly bigger in size, shows a shift of 53 meV.

In Fig. 4 we show a comparison between ZnS and CdS cores with ZnS/CdS and CdS/ZnS core-shell structures. The results are in accord with the experimental data of Ref. [4]: The absorbance changes little between CdS and CdS/ZnS in the low-energy region, but the change is drastic between ZnS and ZnS/CdS. The former result has to do with a surface that is already fully passivated so that a thin barrier shell enhances the localization only slightly. On the other hand, in ZnS/CdS, the outer shell is a well and the spatial distributions are drastically modified, leading to a different absorption spectrum.

To conclude, we have studied the electronic structure and optical properties of spherical nanoheterostructures based on ZnS and CdS within a symmetry-based tight-binding approach. The full single-particle spectrum, the low-energy excitonic states as well as the relative intensities of optical transitions are calculated. A careful analysis of the spatial distribution of the DOS and the HOMO and LUMO wavefunctions reveals that only two monolayers of CdS suffice to trap both the electron and the hole in the well. Our principal results concern the excitonic fine structure yielding the absorption gap and the resonant photoluminescence Stokes shift. Their size and composition dependences have been analyzed on a monolayer scale. We obtain a satisfactory agreement with the available experimental values of the absorption onset without using any adjustable parameter. The predicted Stokes shifts indicate a strong enhancement in the nanoheterostructures as compared to simple nanocrystals.

This work has been supported by the Spanish Ministerio de Ciencia y Tecnología project MAT2002-00699.

- 
- [1] A. Mews, A. V. Kadavanich, U. Banin, and A. P. Alivisatos, *Phys. Rev. B* **53**, R13 242 (1996).
- [2] D. Schooss, A. Mews, A. Eychmüller, and H. Weller, *Phys. Rev. B* **49**, 17 072 (1994).
- [3] F. Koberling, A. Mews, and T. Basché, *Phys. Rev. B* **60**, 1921 (1999).
- [4] R. B. Little, M. A. El-Sayed, G. W. Bryant, and S. Burke, *J. Chem. Phys.* **114**, 1813 (2001).
- [5] C. Ricolleau, L. Audinet, M. Gandais, and T. Gacoin, *Thin Solid Films*, **336**, 213 (1998).
- [6] B. O. Dabbousi, J. Rodriguez-Viejo, F. V. Mikulec, J. R. Heine, H. Mattoussi, R. Ober, K. F. Jensen, and M. G. Bawendi *J. Phys. Chem. B* **101**, 9463 (1997).
- [7] E. Hao, H. P. Sun, Z. Zhou, J. Liu, B. Yang, J. C. Shen, *Chem. Mater.* **11**, 3096 (1999).
- [8] W. Jaskólski and G. W. Bryant, *Phys. Rev. B* **57**, R4237 (1998).
- [9] J. Pérez-Conde and A. K. Bhattacharjee, *phys. stat. sol. (b)* **229**, 485 (2002).
- [10] J. Pérez-Conde and A. K. Bhattacharjee, *Phys. Rev. B* **63**, 245318 (2001).
- [11] J. Pérez-Conde, A. K. Bhattacharjee, M. Chamarro, P. Lavallard, V. D. Petrikov, and A. A. Lipovskii, *Phys. Rev. B* **64**, 113303 (2001).
- [12] J. Pérez-Conde and A. K. Bhattacharjee, *Solid State Comm.* **110**, 259 (1999).
- [13] G. W. Bryant and W. Jaskólski, *phys. stat. sol. (b)* **224**, 751 (2001).
- [14] R.-H. Xie, G. W. Bryant, S. Lee, and W. Jaskolski, *Phys. Rev. B* **65**, 235306 (2002).
- [15] P. Vogl, H. P. Hjalmarson, and J. D. Dow, *J. Phys. Chem. Solids* **44**, 365 (1983).
- [16] A. Kobayashi, O. F. Sankey, and J. D. Dow, *Phys. Rev. B* **25**, 6367 (1982).
- [17] P. E. Lippens and M. Lannoo, *Phys. Rev. B* **39**, 10935 (1989).
- [18] D. Bertho (unpublished), cited by V. Albe, Doctoral thesis, Université Montpellier II (1997).
- [19] G. F. Koster, J. O. Dimmock, R. G. Wheeler and H. Statz, *Properties of the Thirty-Two Point Groups (MIT Press, Cambridge, MA, 1963)*.
- [20] K. Leung, S. Pokrant, and K. B. Whaley, *Phys. Rev. B* **57**, 12 291 (1998).
- [21] L. W. Wang and A. Zunger, *Phys. Rev. B* **53**, 9579 (1996).
- [22] T. B. Boykin, G. Klimeck, R. C. Bowen, and F. Oyafuso, *Phys. Rev. B* **66**, 125207 (2002).

$r_{co}/r_w/r_{cl}$	Core	Well	Clad
7.2/3.2/0.0	0.592(0.323)	0.383(0.671)	0.0(0, 0)
7.2/5.9/0.0	0.322(0.118)	0.659(0.879)	0.0(0.0)
7.2/2.7/2.9	0.419(0.171)	0.328(0.590)	0.241(0.237)
7.2/5.9/2.6	0.211(0.046)	0.623(0.663)	0.158(0.289)

Table I: The probability of presence of electron(hole) in the LUMO(HOMO). The core radius and the well and clad widths are given in the first column for each case (in angstroms).

$r_{co}/r_w/r_{cl}$ (Å)	H1 (eV)	H2 (eV)	L1 (eV)	L2 (eV)
10.1/0.0/0.0	-0.322(8, 7)	-0.378(8, 6)	4.251(6)	4.598(7, 8)
7.2/3.2/0.0	-0.156(8)	-0.167(6)	3.995(6)	4.291(8)
7.2/5.9/0.0	0.056(8)	0.036(6)	3.662(6)	3.922(8)
7.2/2.7/2.9	-0.046(8)	-0.058(6)	3.844(6)	4.112(8)
7.2/5.9/2.6	0.188(8)	0.166(6)	3.574(6)	3.809(8)
0.0/14.8/0.0	-0.247(8)	-0.256(8)	2.988(6)	3.335(8)

Table II: ZnS/CdS/ZnS: Energies of the two highest (lowest) occupied (unoccupied) molecular orbitals, denoted by H1, H2 (L1, L2). The symmetry index  $n$  designating  $\Gamma_n$  is shown in the parenthesis. The size and composition are given in the first column.

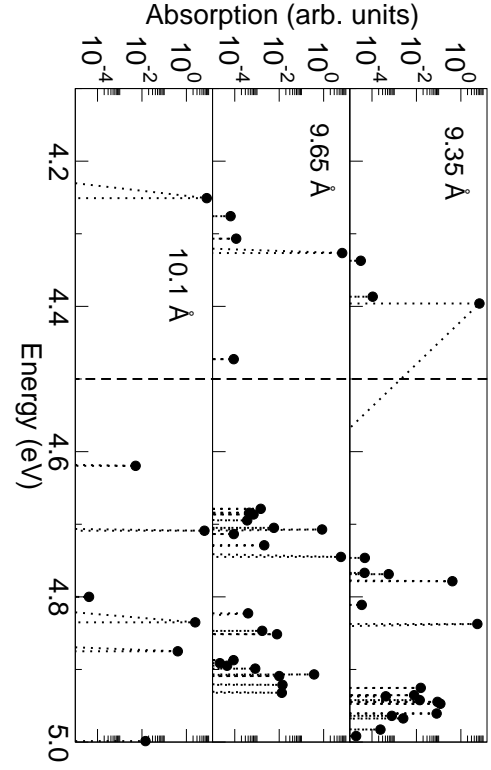


Fig. 2, Perez-Conde, PRB-Brief

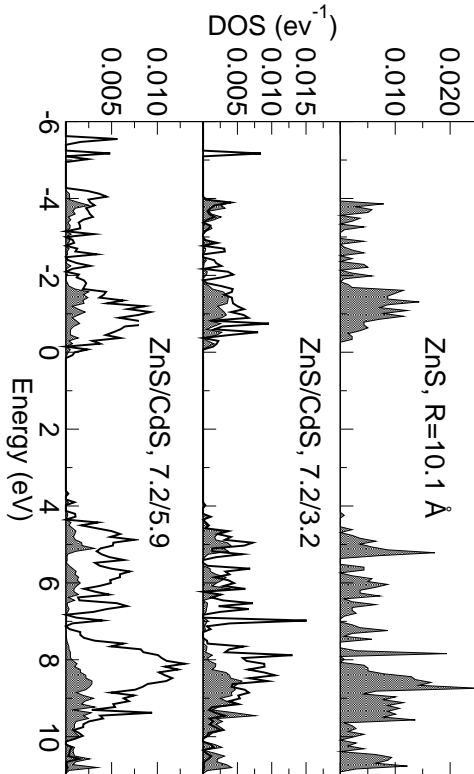


Fig. 1, Perez-Conde, PRB-Brief

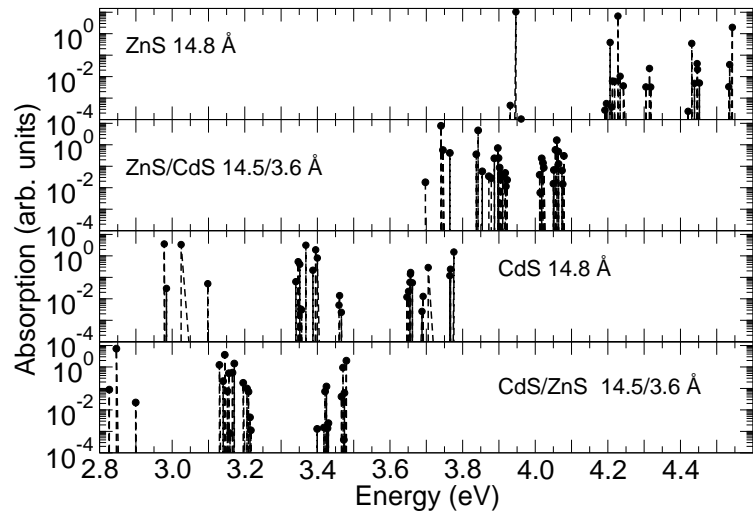


Fig. 4, Perez-Conde, PRB-Brief

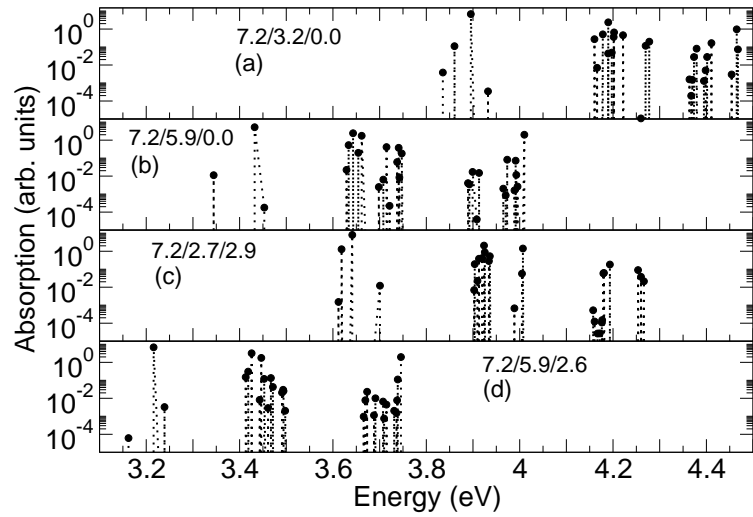


Fig. 3, Perez-Conde, PRB-Brief

Figure 1: Density of States for three NC's. Top: DOS in a ZnS QD of radius  $R = 10.1 \text{ \AA}$ . Middle(bottom): A ZnS/CdS nanocrystal with a core of  $R = 7.2 \text{ \AA}$  and one (two) CdS monolayer (s). In the middle and bottom figures the shaded region corresponds to the DOS projected onto ZnS core region and the solid line to the DOS projected onto the CdS well region.

Figure 2: Excitonic fine structure in ZnS QD's. The experimental absorption onset is indicated by the vertical dashed line. We show three similar sized QD's of around  $10 \text{ \AA}$  in radius.

Figure 3: Excitonic fine structure in QDQW's. The core radii and shell thickness are all given in  $\text{\AA}$ . The respective experimental absorption onsets are: (a)  $3.85 \text{ eV}$ , (b)  $3.55 \text{ eV}$ , (c)  $3.76 \text{ eV}$ , (d)  $3.45 \text{ eV}$ .

Figure 4: Excitonic fine structure in core and core-shell nanostructures. The core radii and shell thickness are all given in  $\text{\AA}$ .